Augerの最近の異方性解析について

Observation of a large-scale anisotropy in the arrival directions of cosmic rays above 8×10^{18} eV
Pierre Auger Collaboration, Science 357, 1266 (2017)

Indication of anisotropy in arrival directions of ultra-high-energy cosmic rays through comparison to the flux pattern of extragalactic gamma-ray sources
Pierre Auger Collaboration, Astrophys.J. 853 (2018) L29

藤井 俊博　fujii@icrr.u-tokyo.ac.jp

第2回 空気シャワー観測による宇宙線の起源探索勉強会

2018年2月26日

1

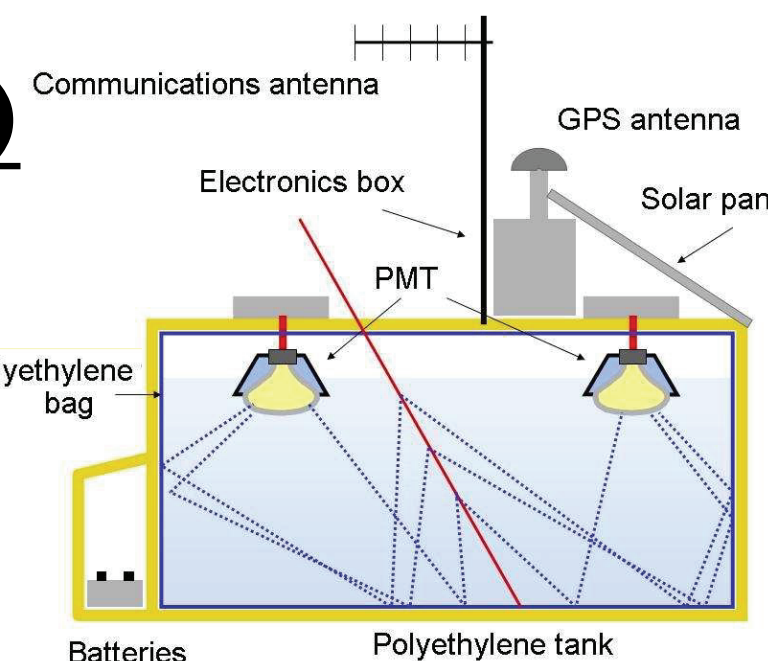# Pierre Auger Observatory (Auger)

The world's largest UHECR observatory 3000 km^2

(2004 -) completed in 2008
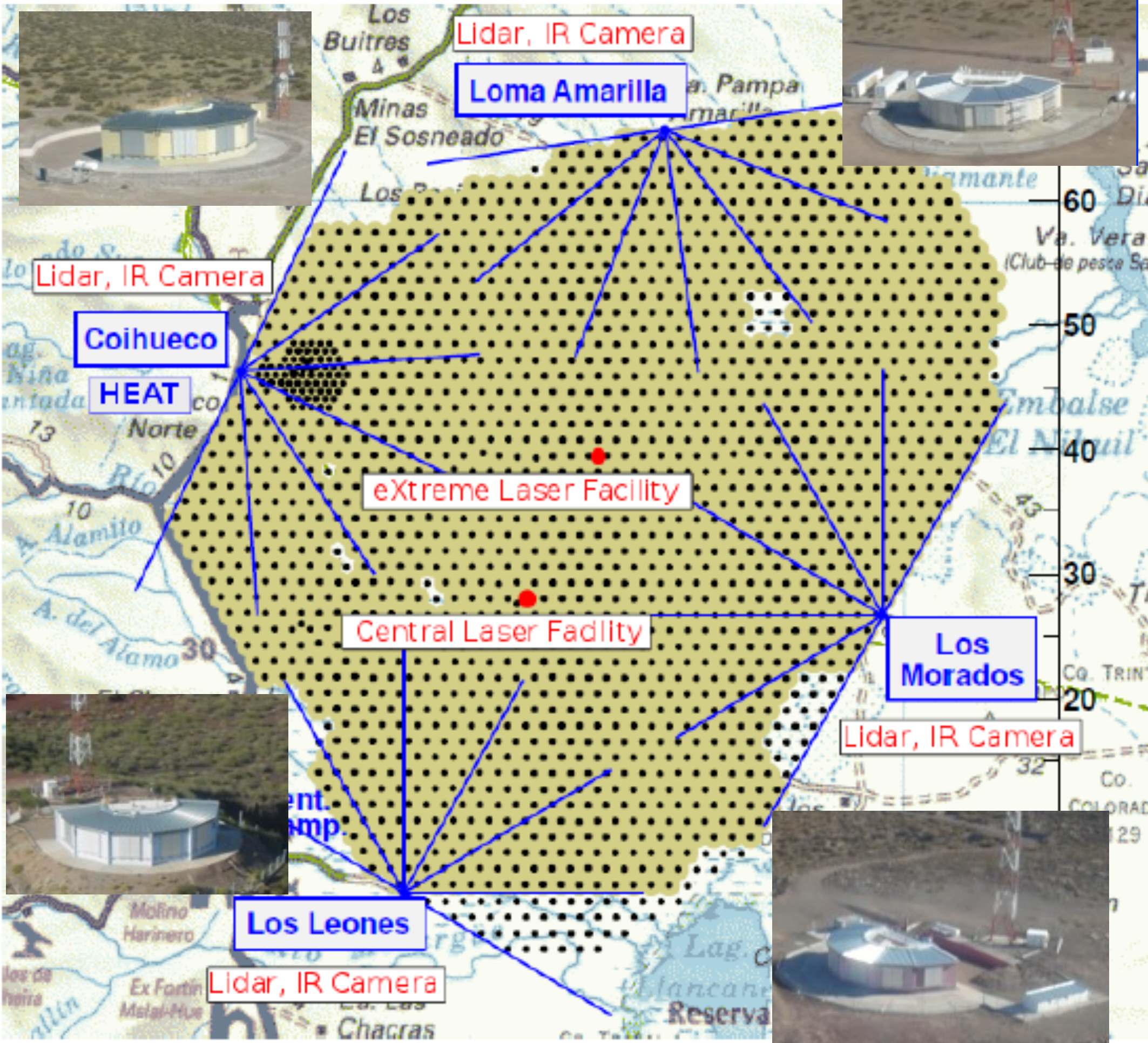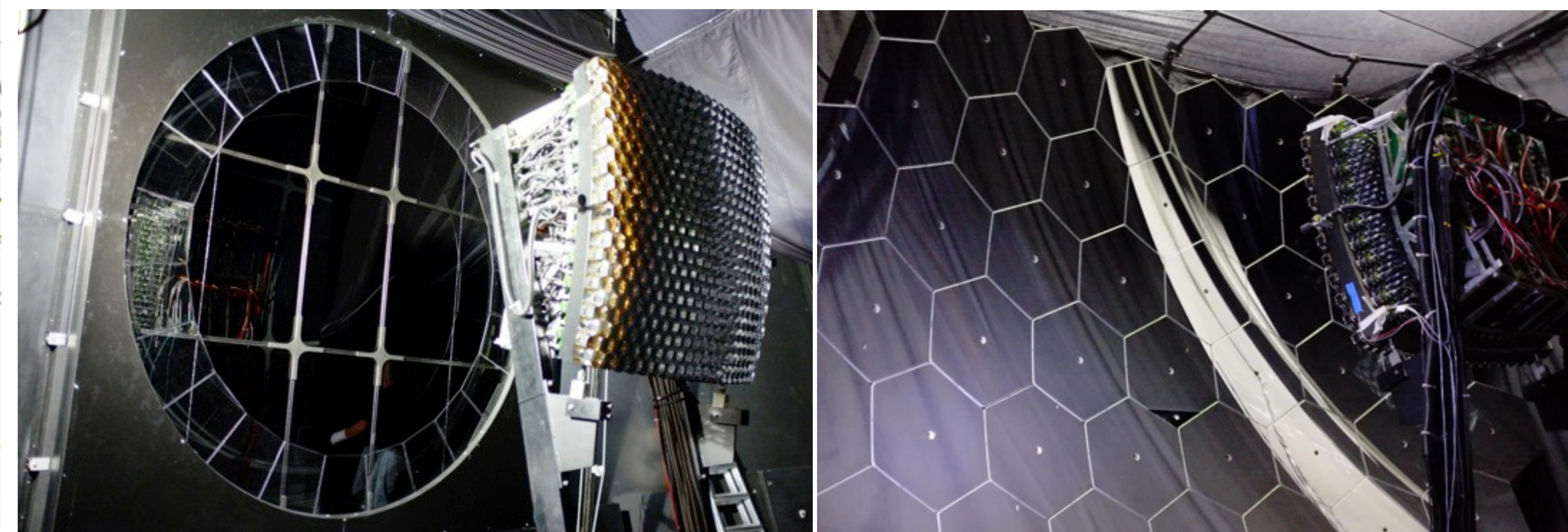

Surface Detector (SD)

Water Cherenkov Tank
1.5 km spacing, 1600
stations, 10 m^2
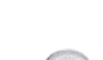
Fluorescence Detector (FD)

3.4 m spherical mirror, 440 PMT, 30° × 30° FOV
light guide + collector ring, 4 × 6 telescope

Malargüe, Mendoza, Argentina

An observation of a dipole above 8 EeV

PIERRE
AUGER
OBSERVATORY

- Jan/2004 – Aug/2016

- Zenith < 80° → covering 85% of the sky

- $E > 4$ EeV → full trigger efficiency

Harmonic analysis in right ascension α

E [EeV]	events	amplitude r	phase [deg.]	$P(\geq r)$
4-8	81701	$0.005^{+0.006}_{-0.002}$	80 ± 60	0.60
> 8	32187	$0.047^{+0.008}_{-0.007}$	100 ± 10	2.6×10^{-8}

significant modulation at 5.2σ (5.6σ before penalization for energy bins explored)

E > 8 EeV

Galactic center

data E>8 EeV
first harmonic
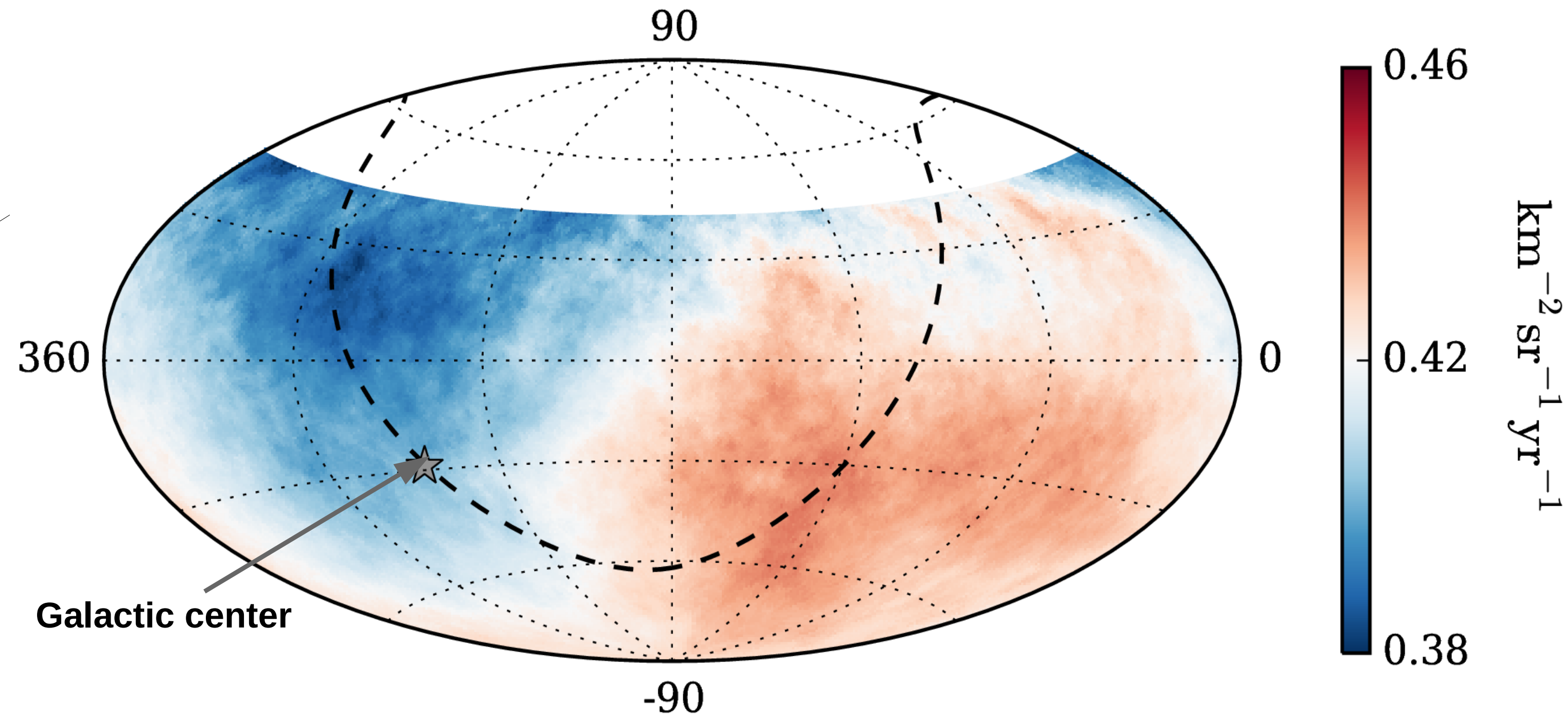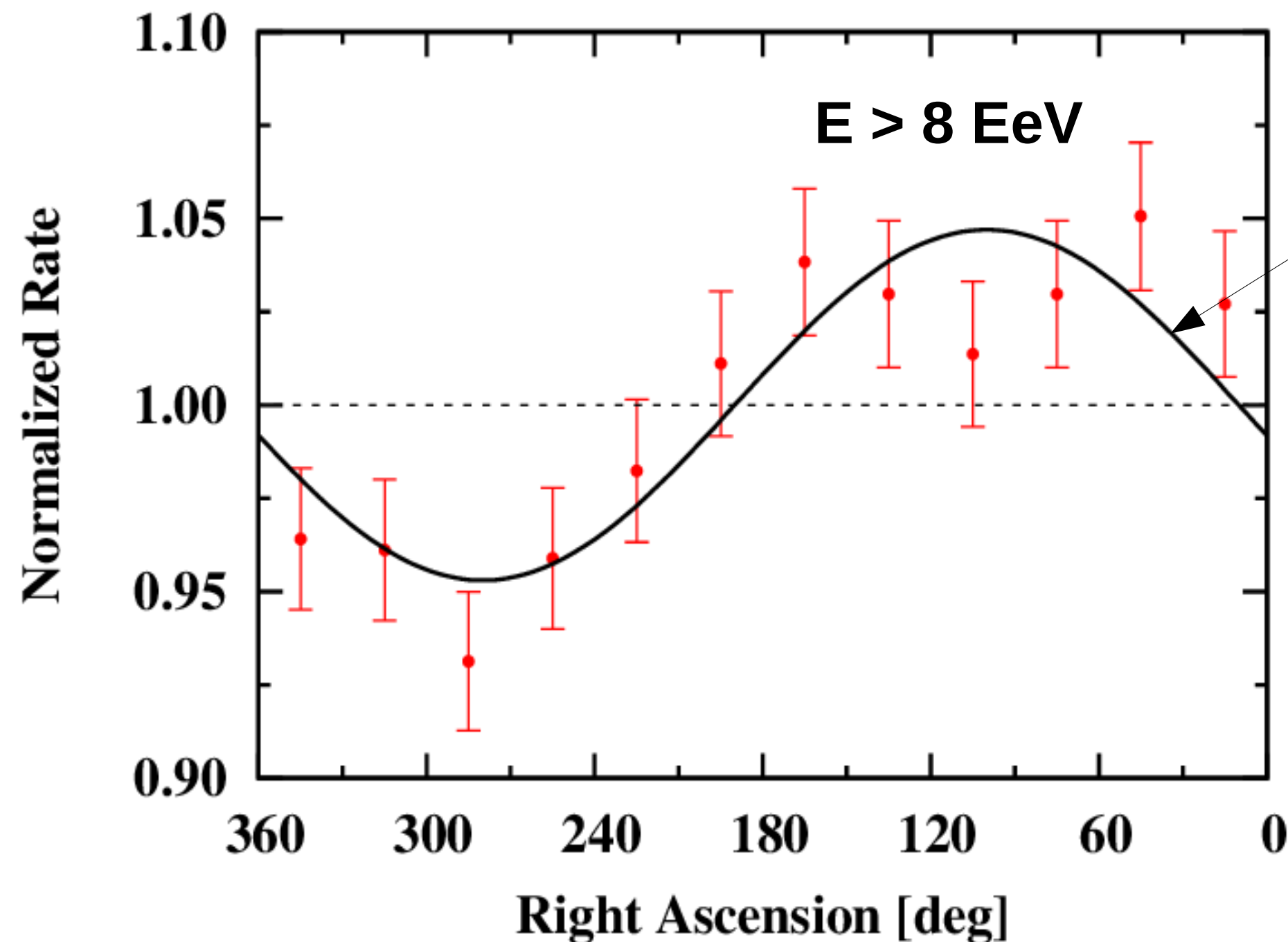
A directional reconstruction of the dipole

E [EeV]	d_z [%]	$d_\perp$ [%]	d [%]	$\delta_{\mathrm{d}}[°]$	$\alpha_{\mathrm{d}}[°]$
4 - 8	-2.4 ± 0.9	$0.6^{+0.7}_{-0.3}$	$2.5^{+1.0}_{-0.7}$	-75^{+17}_{-8}	80 ± 60
≥ 8	-2.6 ± 1.5	$6.0^{+1.1}_{-1.0}$	$6.5^{+1.3}_{-0.9}$	-24^{+12}_{-13}	100 ± 10

6.5% dipole amplitude
Equatorial $(\alpha_{\mathrm{d}}, \delta_{\mathrm{d}}) = (100°, -24°)$
Galactic $(l, b) = (233°, -13°)$
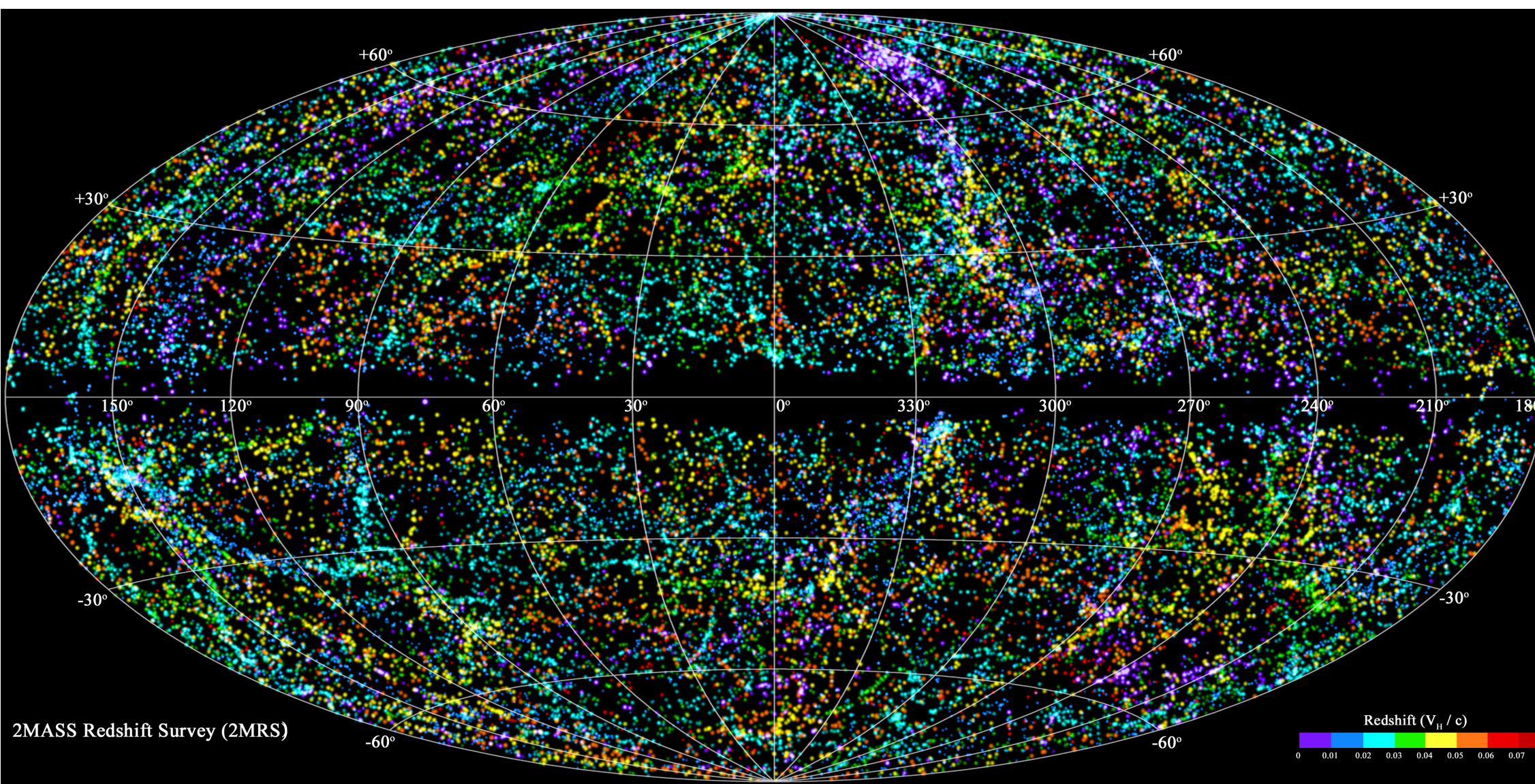
The flux-weighted dipole from IR galaxy distribution in

2MRS points to (l,b)=(251º,38º) → **~55º from observed**

[Erdogdu et al. 2006]

2MASS redshift survey
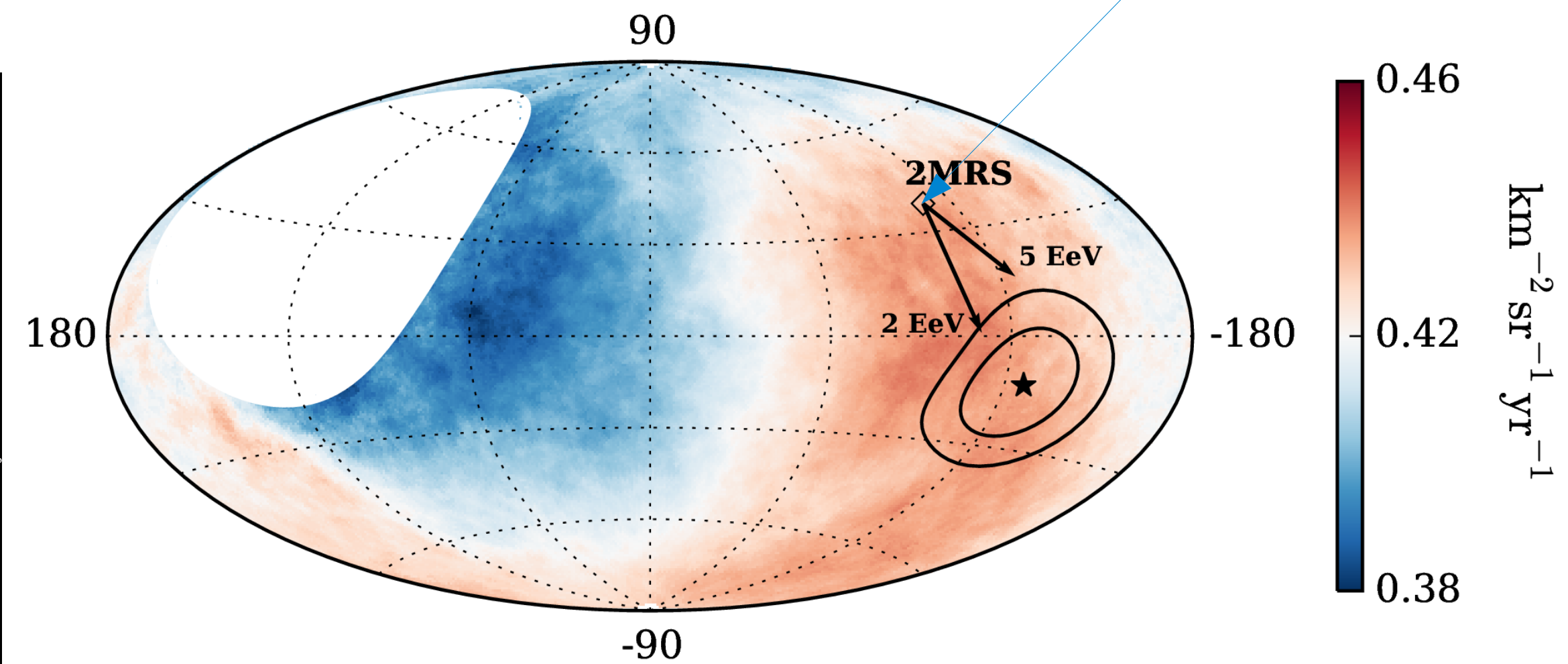
Accounting GMF deflections

[Jansson and Farrar ApJ 757 (2012) 14]

Z ~ 1.7 – 5 at 10 EeV ⟶ **E/Z ~ 2 – 5 EeV**

[Auger Coll. PRD 90 (2014) 122006]

Improves agreement observation ↔ 2MRS

O. Taborda et al., ICRC 2017

5

A prediction of the dipole amplitude

0 - 50 Mpc

proton inj., $\gamma = 2.6$

50 - 100 Mpc

0.06   0.08   0.1

$\Phi(\hat{\mathbf{n}}, E > 10\,\mathrm{EeV})\,[\mathrm{sr}^{-1}]$

silicon inj., $\gamma = 1.5$
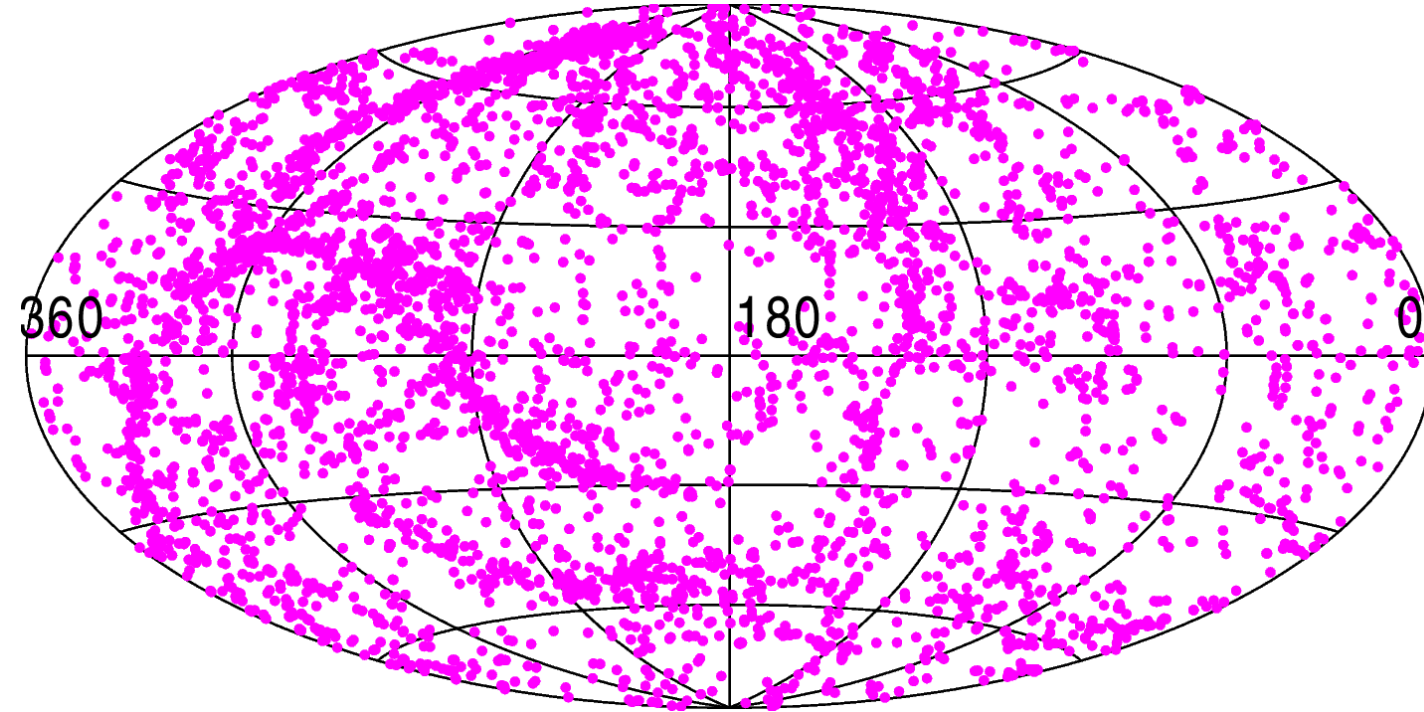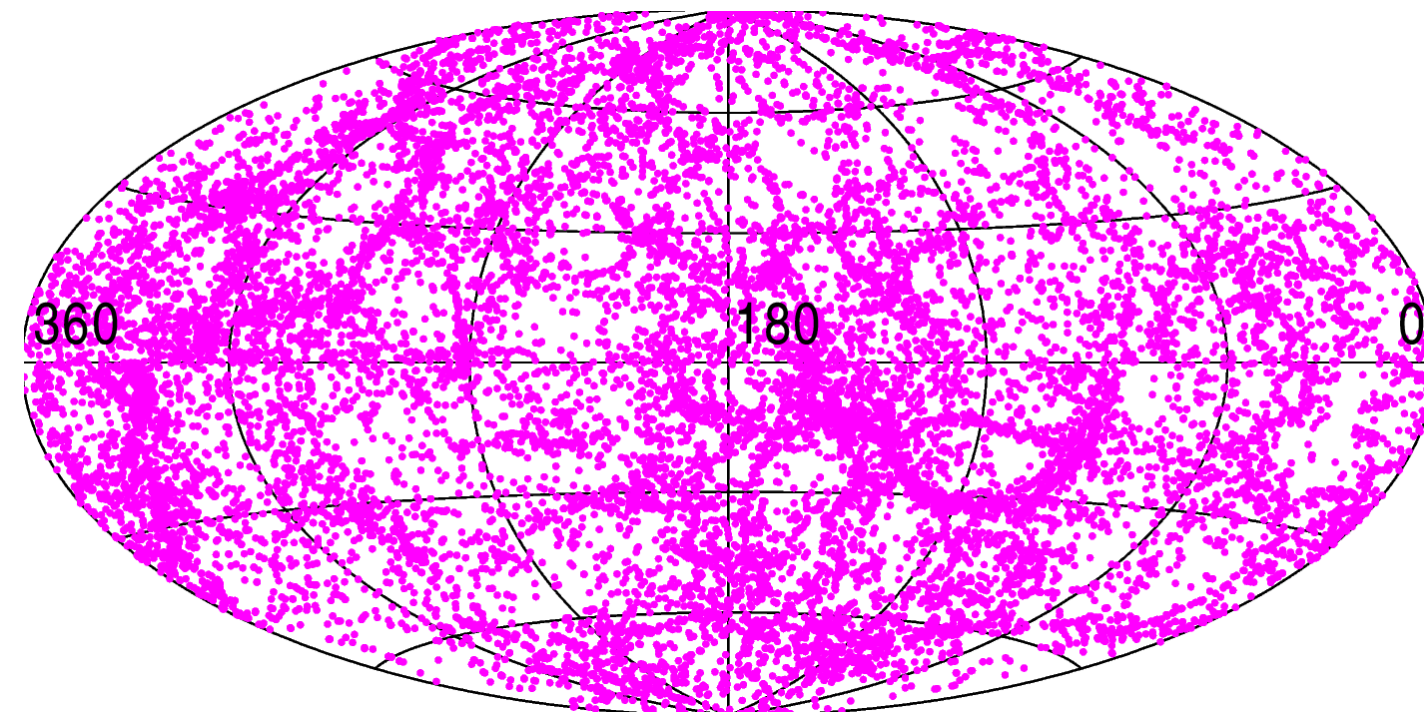
100 - 250 Mpc
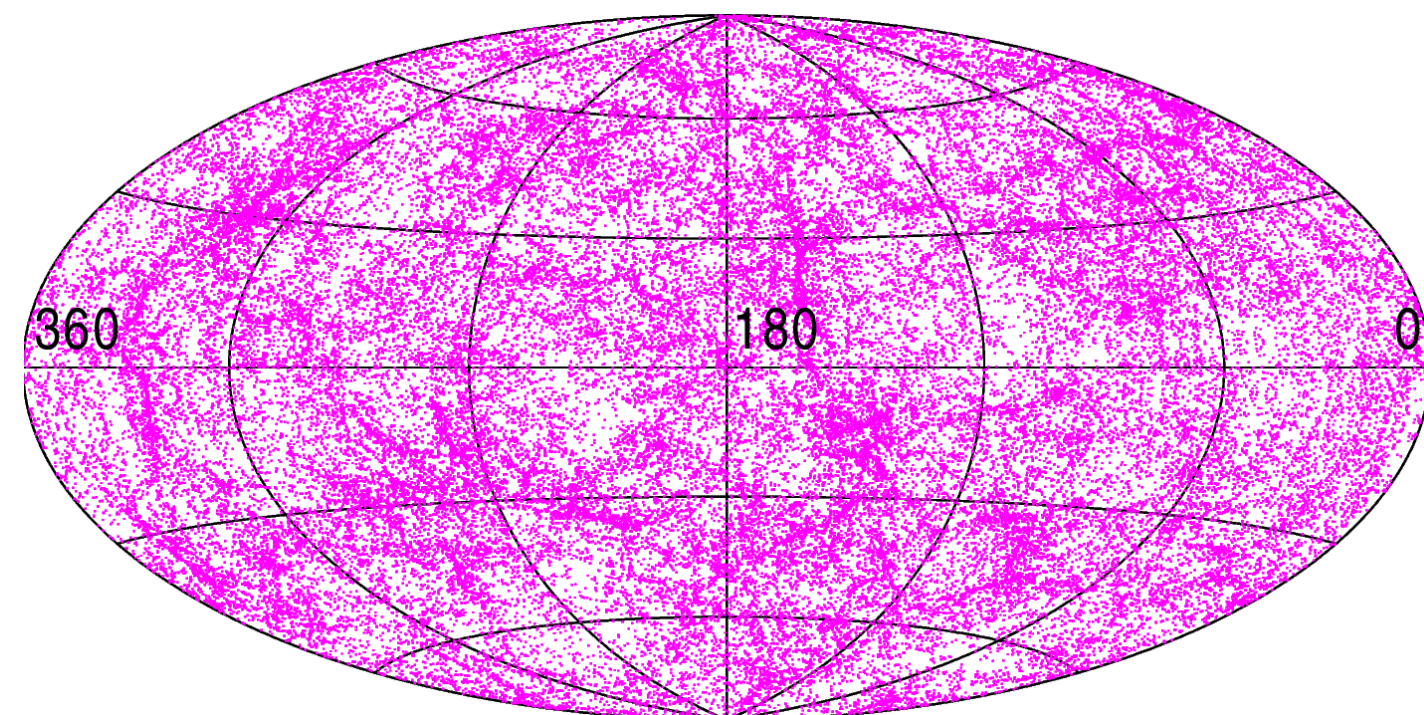
遠くまで見えると等方的に天体が分布

(2MASS Redshift survey galaxies)
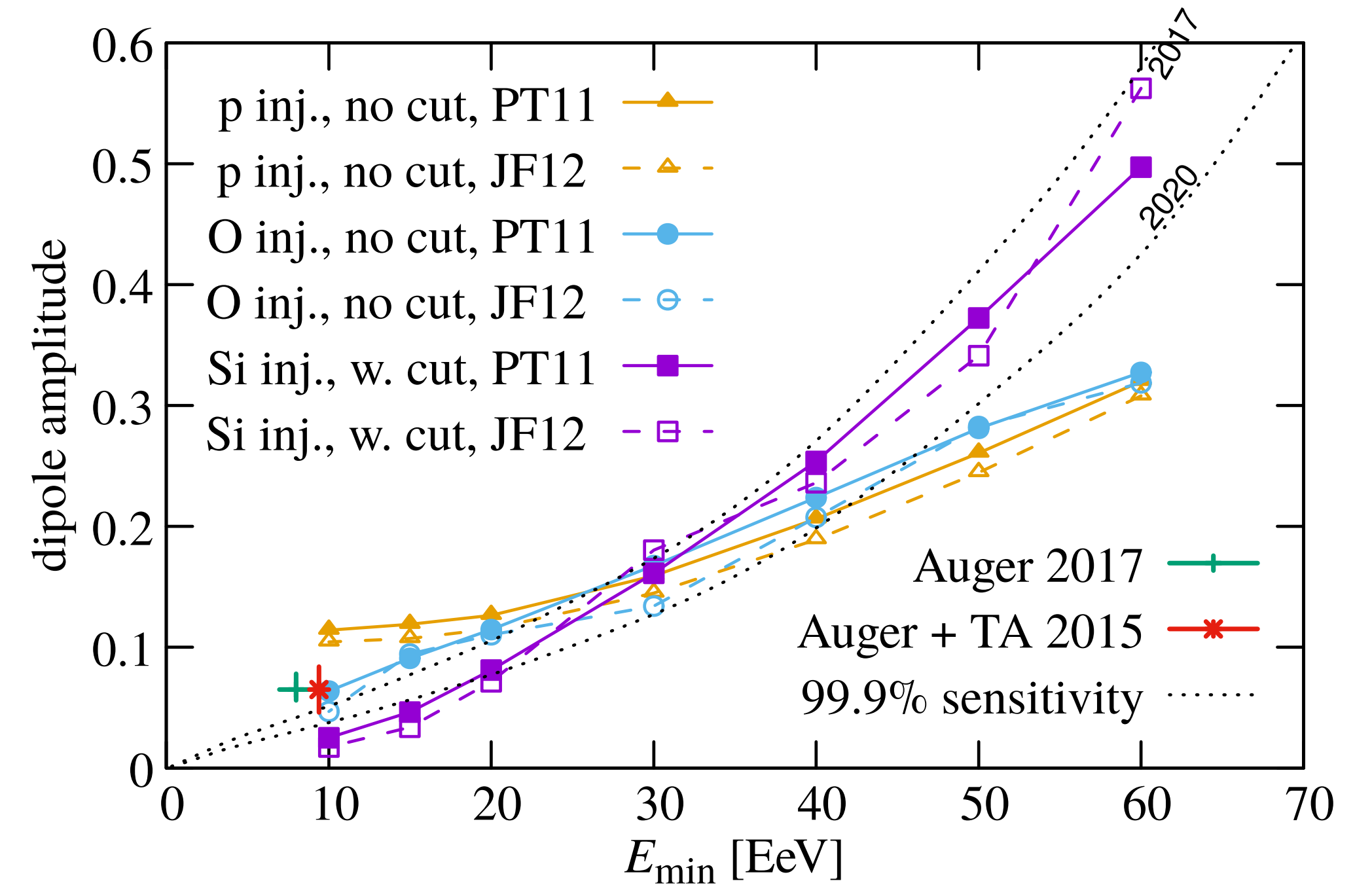
Figure 6. The magnitude of the dipole as a function of the energy threshold $E_{\min}$ for the three injection models and two GMF models we considered. The points labelled "Auger + TA 2015" and "Auger 2017" show the dipole magnitude reported in Deligny (2015) and Taborda (2017) respectively. The dotted lines show the 99.9% C.L. detection thresholds using the current and near-future Auger and TA exposures (see the text for details).

Amplitudeが陽子+銀河磁場から期待される値より小さい

INDICATION OF ANISOTROPY IN ARRIVAL DIRECTIONS OF ULTRA-HIGH-ENERGY COSMIC RAYS THROUGH COMPARISON TO THE FLUX PATTERN OF EXTRAGALACTIC GAMMA-RAY SOURCES

THE PIERRE AUGER COLLABORATION

(See the end matter for the full list of authors.)

ABSTRACT

A new analysis of the dataset from the Pierre Auger Observatory provides evidence for anisotropy in the arrival directions of ultra-high-energy cosmic rays on an intermediate angular scale, which is indicative of excess arrivals from strong, nearby sources. The data consist of 5514 events above 20 EeV with zenith angles up to 80° recorded before 2017 April 30. Sky models have been created for two distinct populations of extragalactic gamma-ray emitters: active galactic nuclei from the second catalog of hard *Fermi*-LAT sources (2FHL) and starburst galaxies from a sample that was examined with *Fermi*-LAT. Flux-limited samples, which include all types of galaxies from the *Swift*-BAT and 2MASS surveys, have been investigated for comparison. The sky model of cosmic-ray density constructed using each catalog has two free parameters, the fraction of events correlating with astrophysical objects and an angular scale characterizing the clustering of cosmic rays around extragalactic sources. A maximum-likelihood ratio test is used to evaluate the best values of these parameters and to quantify the strength of each model by contrast with isotropy. It is found that the starburst model fits the data better than the hypothesis of isotropy with a statistical significance of $4.0\,\sigma$, the highest value of the test statistic being for energies above 39 EeV. The three alternative models are favored against isotropy with $2.7-3.2\,\sigma$ significance. The origin of the indicated deviation from isotropy is examined and prospects for more sensitive future studies are discussed.

Keywords: astroparticle physics — cosmic rays — galaxies: active — galaxies: starburst — methods: data analysis

Starburst galaxy (SBGs)

M82 X-1: 100-10000 Ms BH

NGC253

M82

NGC4945

NGC1068

M83
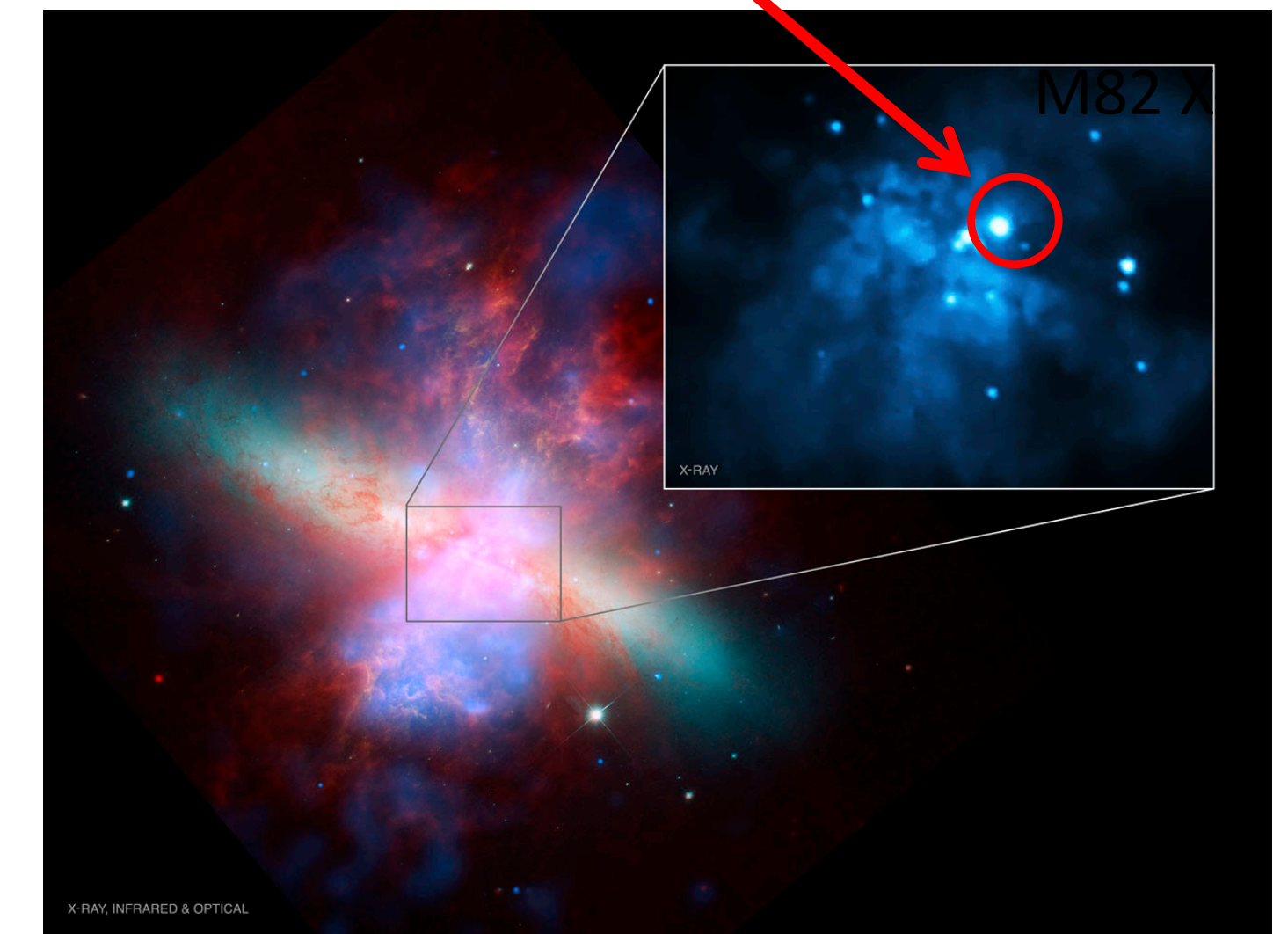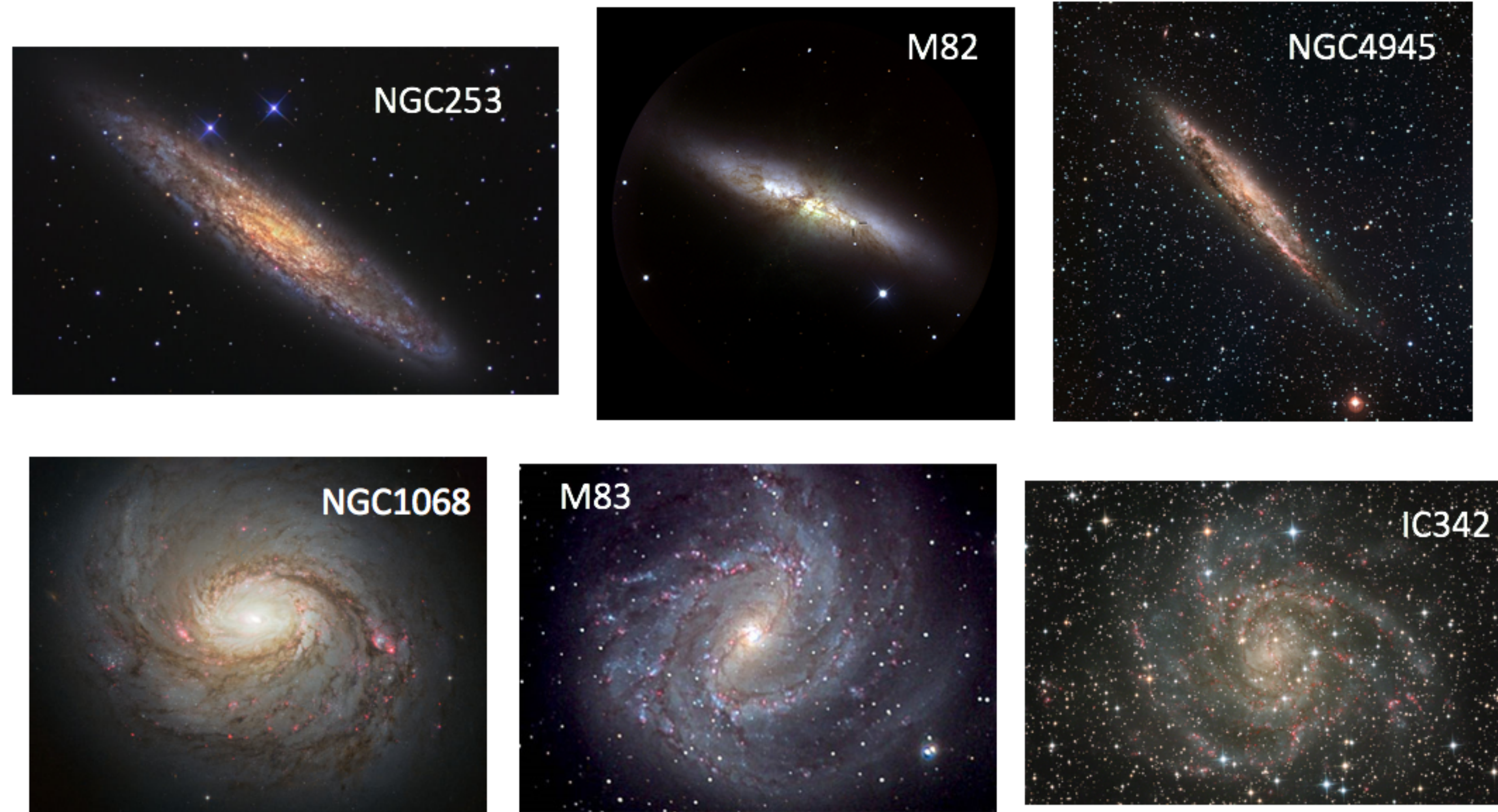
Composite of X-ray, IR, and optical emissions

NASA / CXC / JHU / D. Strickland; optical: NASA / ESA / STScI / AURA/ Hubble Heritage Team; IR: NASA / JPL-Caltech /Univ. of AZ / C. Engelbracht; inset – NASA / CXC / Tsinghua University / H. Feng et al.
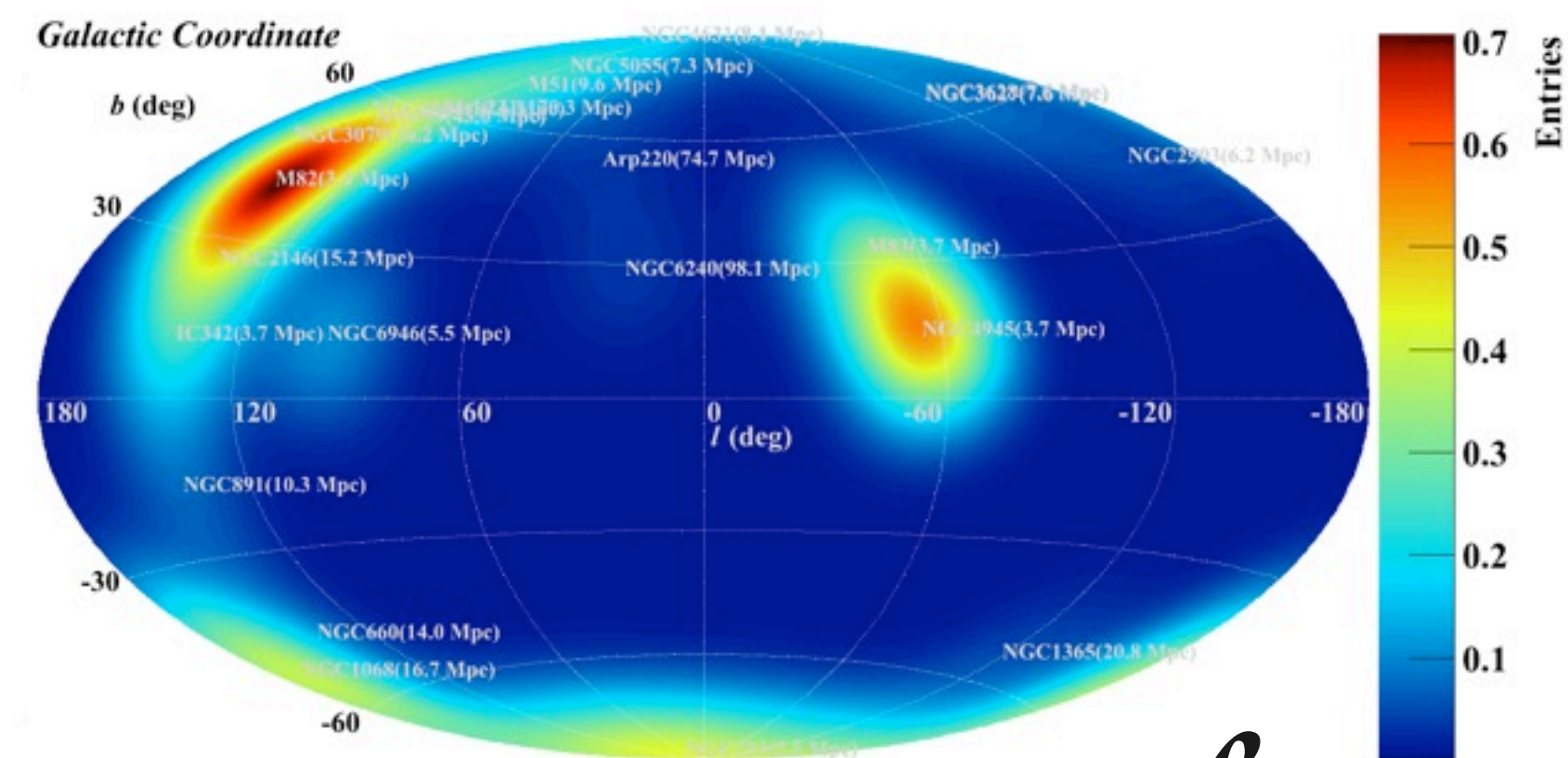
✦ 典型的な銀河に比べて星形成率が100~1000倍大きい

✦ 活動銀河核とは違って、中心に10^7-10^8太陽質量の大質量ブラックホールがない
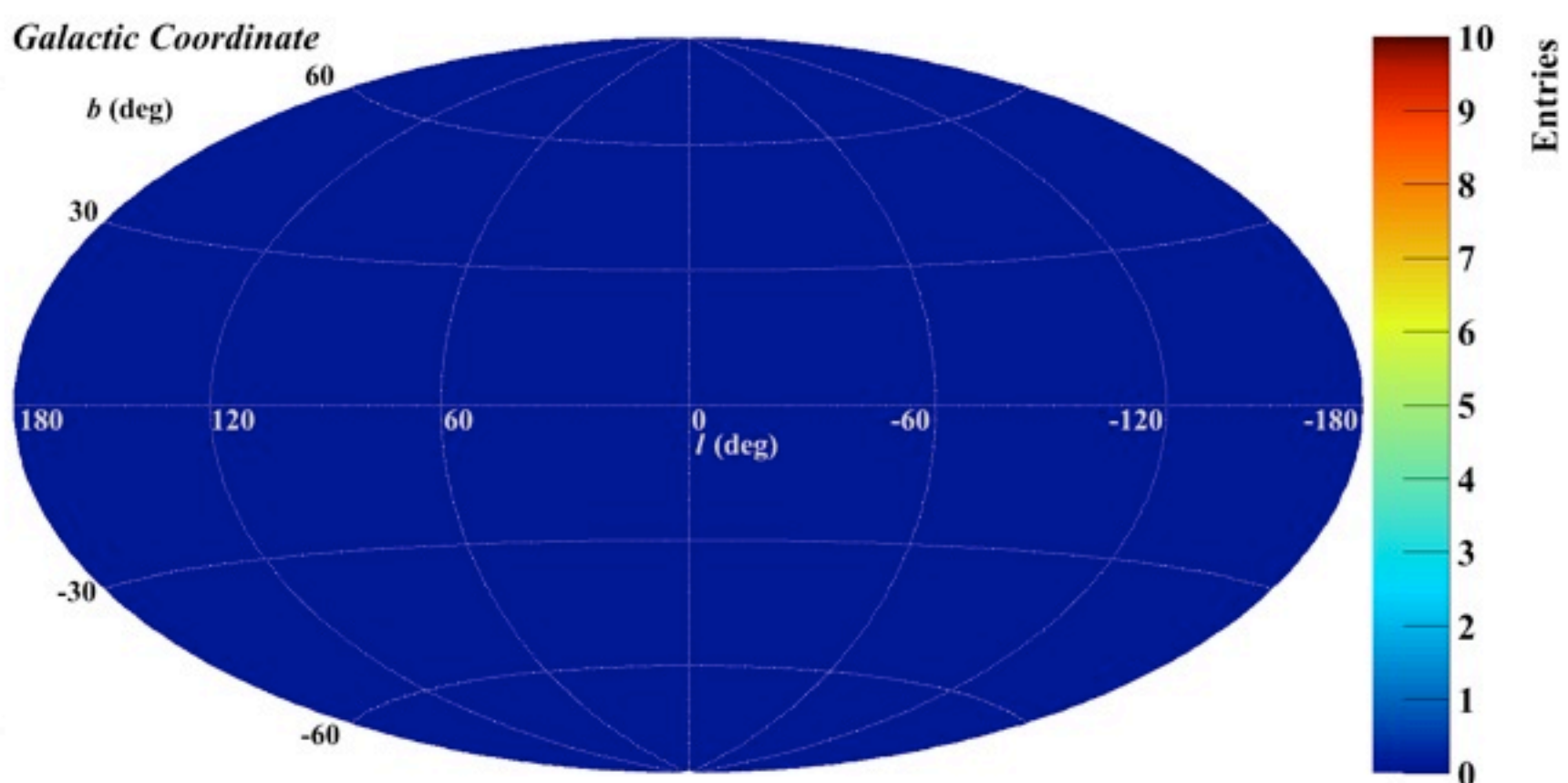
　✦ ガンマ線バーストや活動銀河核に比べると、宇宙線を極高エネルギーまで加速するのは難しそう

UHECRとFlux patternの相関解析

Assumption: UHECRs flux proportional to non-thermal photon

SBGs flux pattern

+

×f_{ani}

×(1- f_{ani})

Exposure at Auger
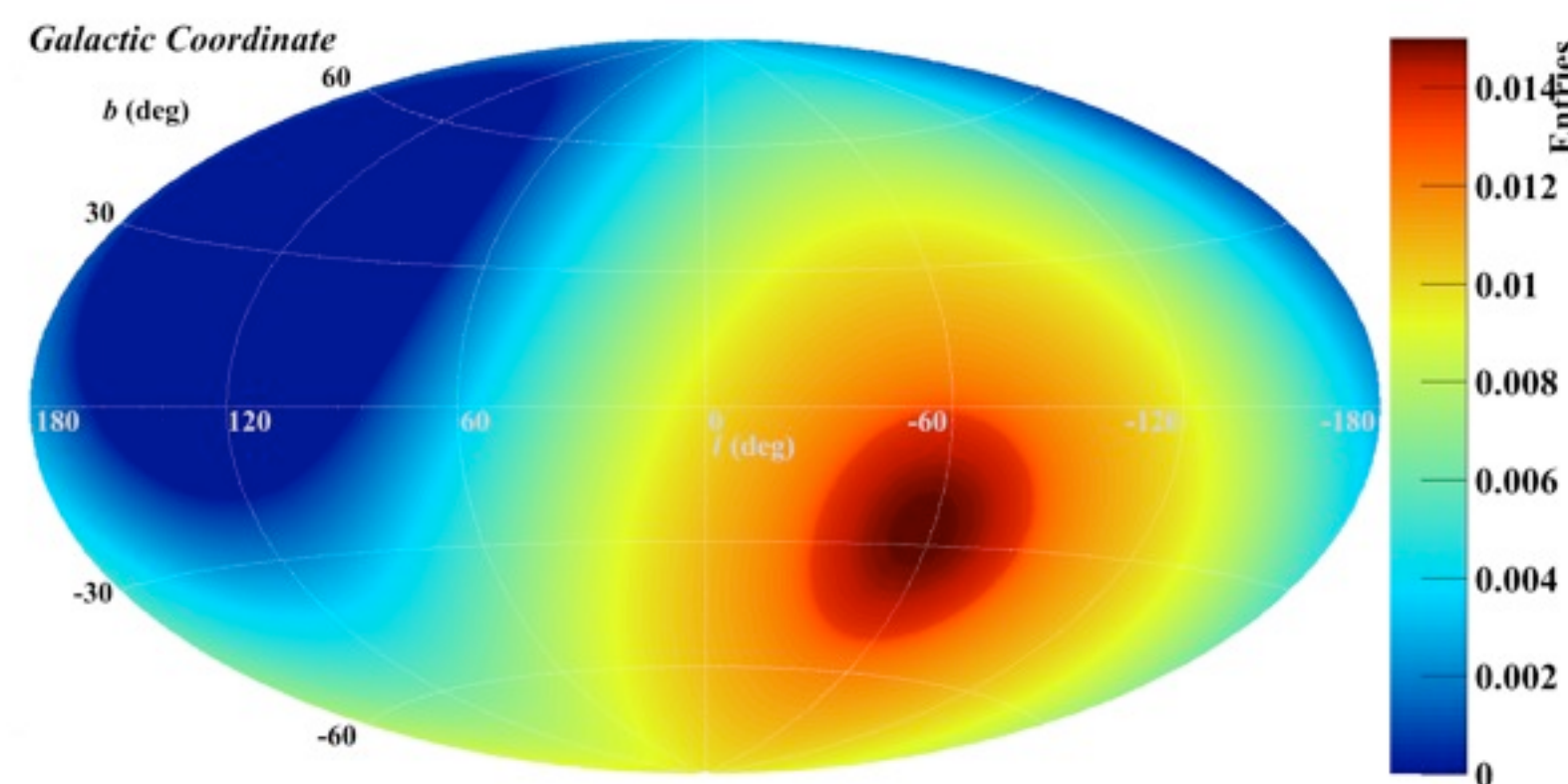
Flux pattern at Auger
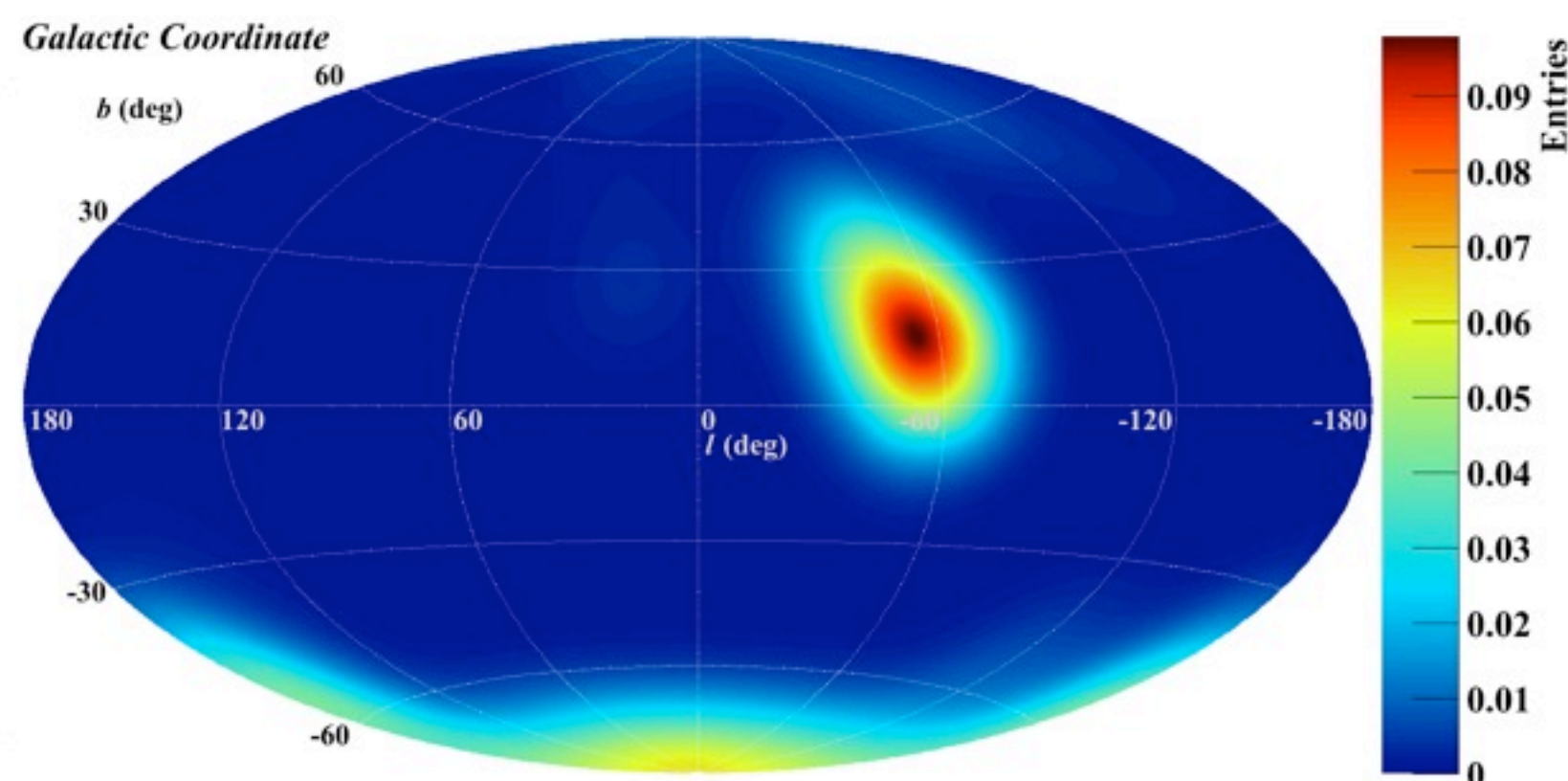
$$TS = 2\log\left[\frac{L(\phi, f_{\mathrm{ani}})}{L(f_{\mathrm{ani}} = 0)}\right]$$

✦ Energy scan from 20 - 80 EeV

✦ Φ : angular scale (width of gaussian)

✦ f_{ani} : anisotropic fraction

✦ L : likelihood from a model map

  ✦ $L(\Phi, f_{\mathrm{ani}})$ = (1 - f_{ani}) × isotropy + f_{ani} × fluxMap(Φ)

  ✦ $L(f_{\mathrm{ani}}$=0): isotropy

An attenuation factor of the flux map

Scenario A: EPOS-LHC, hard injection γ=1.0

Scenario B: EPOS-LHC, γ=2.0

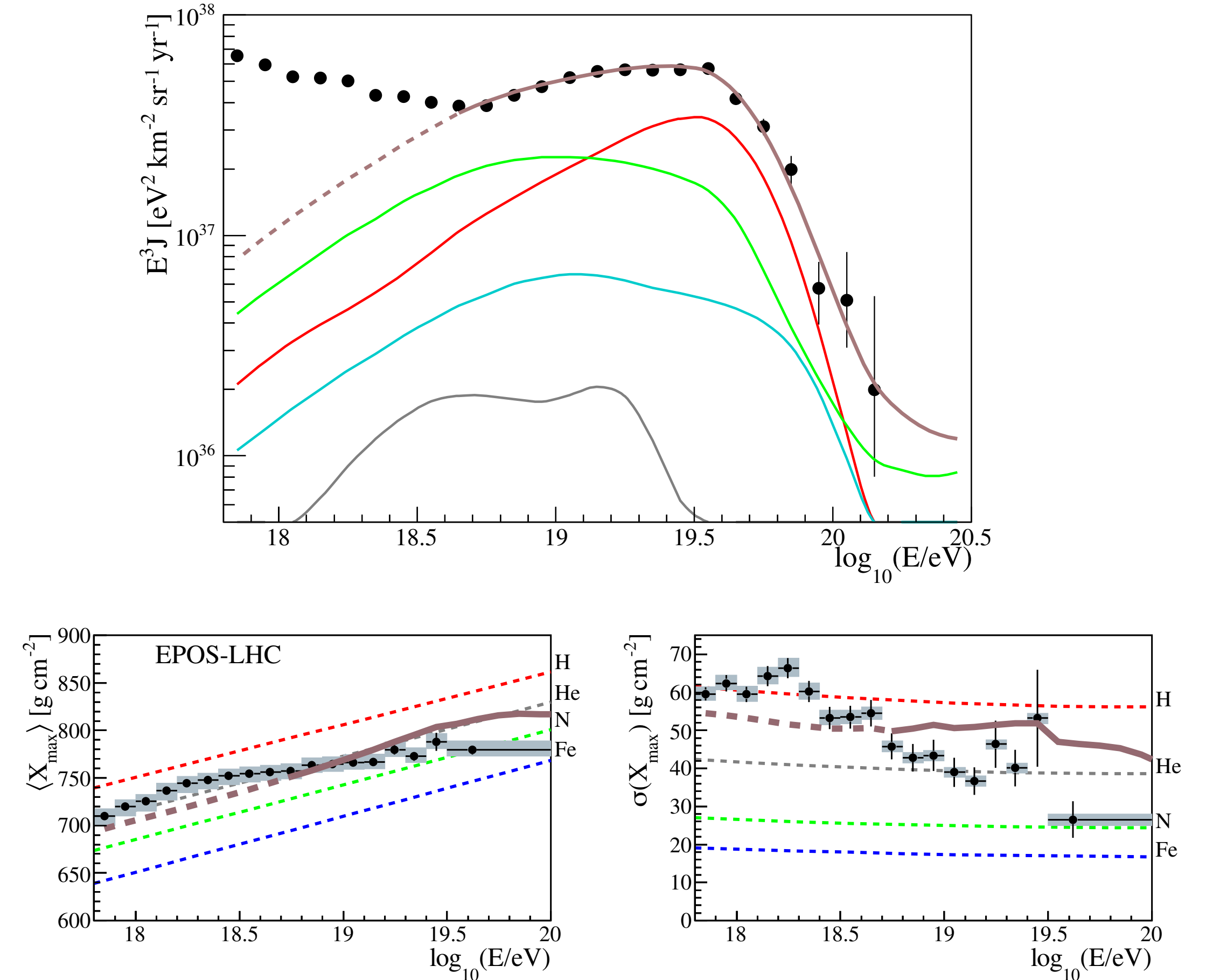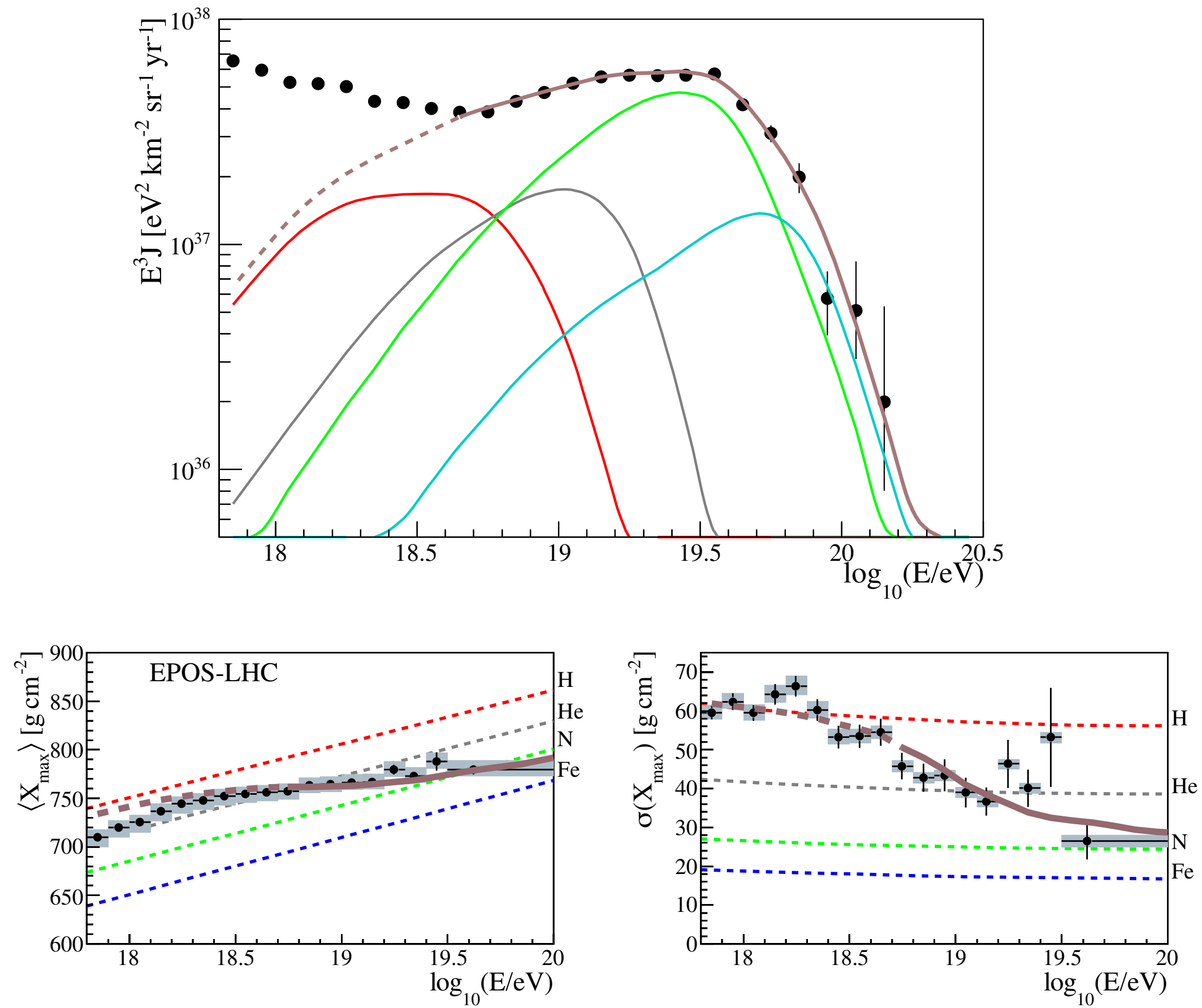**Figure 3**. Top: simulated energy spectrum of UHECRs (multiplied by E^3) at the top of the Earth's atmosphere, obtained with the best-fit parameters for the reference model using the procedure described in section 3. Partial spectra are grouped as in figure 2. For comparison the fitted spectrum is reported together with the spectrum in [4] (filled circles). Bottom: average and standard deviation of the X_{max} distribution as predicted (assuming EPOS-LHC UHECR-air interactions) for the model (brown) versus pure ^{1}H (red), ^{4}He (grey), ^{14}N (green) and ^{56}Fe (blue), dashed lines. Only the energy range where the brown lines are solid is included in the fit.

Figure 4. Same as figure 3 at the local minimum at $\gamma = 2.04$, SPG propagation model, EPOS-LHC UHECR-air interactions.

Table 2. Populations investigated

SBGs	l [°]	b [°]	Distance[a] [Mpc]	Flux weight [%]	Attenuated weight: A / B / C [%]	% contribution[b]: A / B / C [%]
NGC 253	97.4	-88	2.7	13.6	20.7 / 18.0 / 16.6	35.9 / 32.2 / 30.2
M82	141.4	40.6	3.6	18.6	24.0 / 22.3 / 21.4	0.2 / 0.1 / 0.1
NGC 4945	305.3	13.3	4	16	19.2 / 18.3 / 17.9	39.0 / 38.4 / 38.3
M83	314.6	32	4	6.3	7.6 / 7.2 / 7.1	13.1 / 12.9 / 12.9
IC 342	138.2	10.6	4	5.5	6.6 / 6.3 / 6.1	0.1 / 0.0 / 0.0
NGC 6946	95.7	11.7	5.9	3.4	3.2 / 3.3 / 3.5	0.1 / 0.1 / 0.1
NGC 2903	208.7	44.5	6.6	1.1	0.9 / 1.0 / 1.1	0.6 / 0.7 / 0.7
NGC 5055	106	74.3	7.8	0.9	0.7 / 0.8 / 0.9	0.2 / 0.2 / 0.2
NGC 3628	240.9	64.8	8.1	1.3	1.0 / 1.1 / 1.2	0.8 / 0.9 / 1.1
NGC 3627	242	64.4	8.1	1.1	0.8 / 0.9 / 1.1	0.7 / 0.8 / 0.9
NGC 4631	142.8	84.2	8.7	2.9	2.1 / 2.4 / 2.7	0.8 / 0.9 / 1.1
M51	104.9	68.6	10.3	3.6	2.3 / 2.8 / 3.3	0.3 / 0.4 / 0.5
NGC 891	140.4	-17.4	11	1.7	1.1 / 1.3 / 1.5	0.2 / 0.3 / 0.3
NGC 3556	148.3	56.3	11.4	0.7	0.4 / 0.6 / 0.6	0.0 / 0.0 / 0.0
NGC 660	141.6	-47.4	15	0.9	0.5 / 0.6 / 0.8	0.4 / 0.5 / 0.6
NGC 2146	135.7	24.9	16.3	2.6	1.3 / 1.7 / 2.0	0.0 / 0.0 / 0.0
NGC 3079	157.8	48.4	17.4	2.1	1.0 / 1.4 / 1.5	0.1 / 0.1 / 0.1
NGC 1068	172.1	-51.9	17.9	12.1	5.6 / 7.9 / 9.0	6.4 / 9.4 / 10.9
NGC 1365	238	-54.6	22.3	1.3	0.5 / 0.8 / 0.8	0.9 / 1.5 / 1.6
Arp 299	141.9	55.4	46	1.6	0.4 / 0.7 / 0.6	0.0 / 0.0 / 0.0
Arp 220	36.6	53	80	0.8	0.1 / 0.3 / 0.2	0.0 / 0.2 / 0.1
NGC 6240	20.7	27.3	105	1	0.1 / 0.3 / 0.1	0.1 / 0.3 / 0.1
Mkn 231	121.6	60.2	183	0.8	0.0 / 0.1 / 0.0	0.0 / 0.0 / 0.0

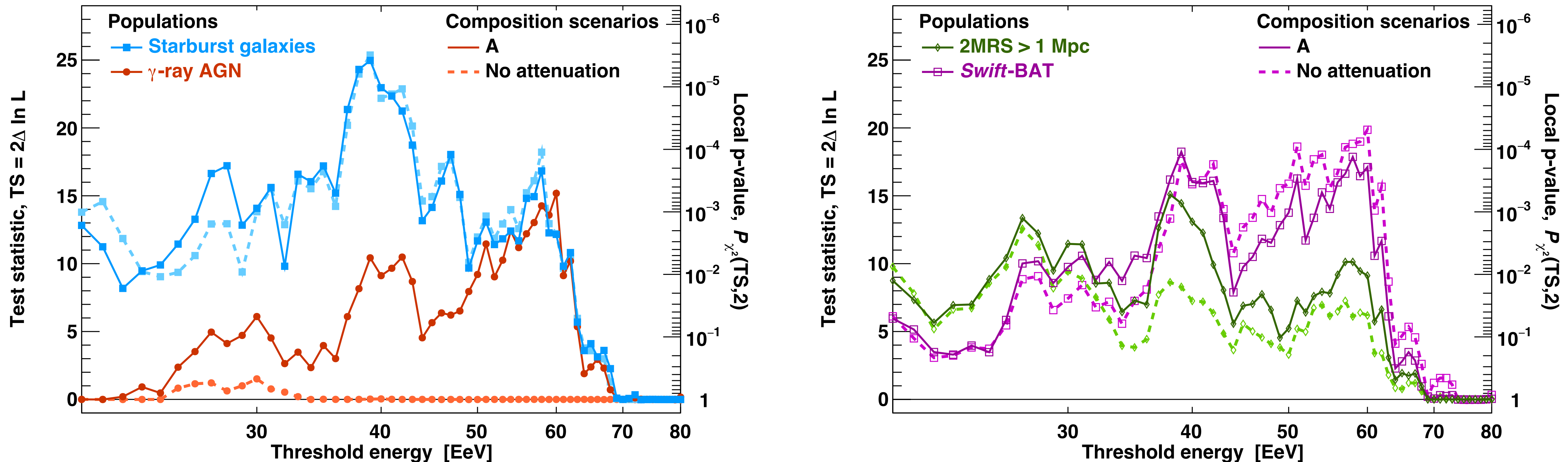# Results of the correlation analysis

Figure 1. TS scan over the threshold energy for SBGs and AGNs (*Left*) and *Swift*-BAT and 2MRS sources (*Right*), including attenuation (light-dashed lines) or not (darker-solid lines).

✦ 40 EeV付近でどのカタログも相関が強くなる
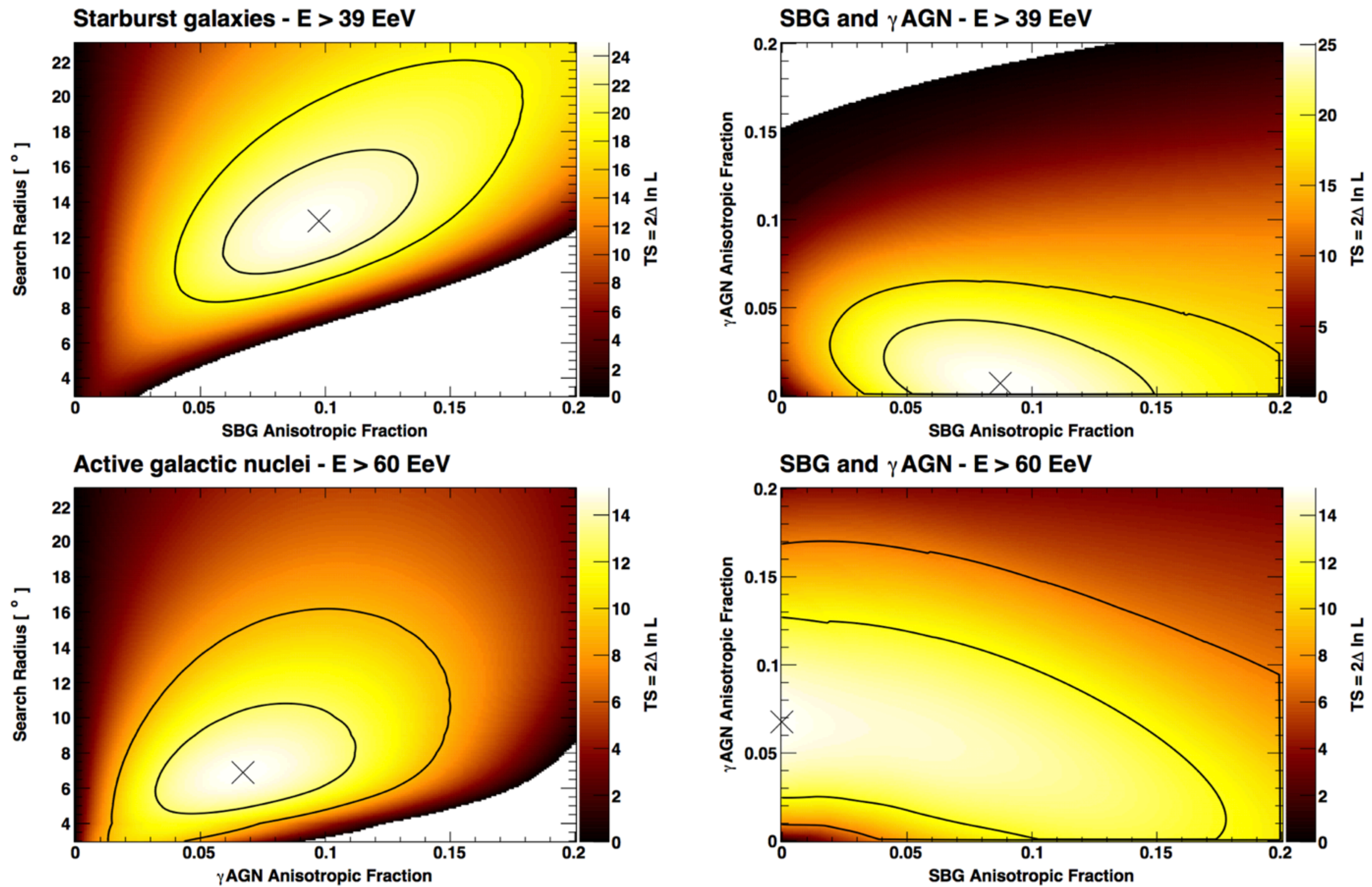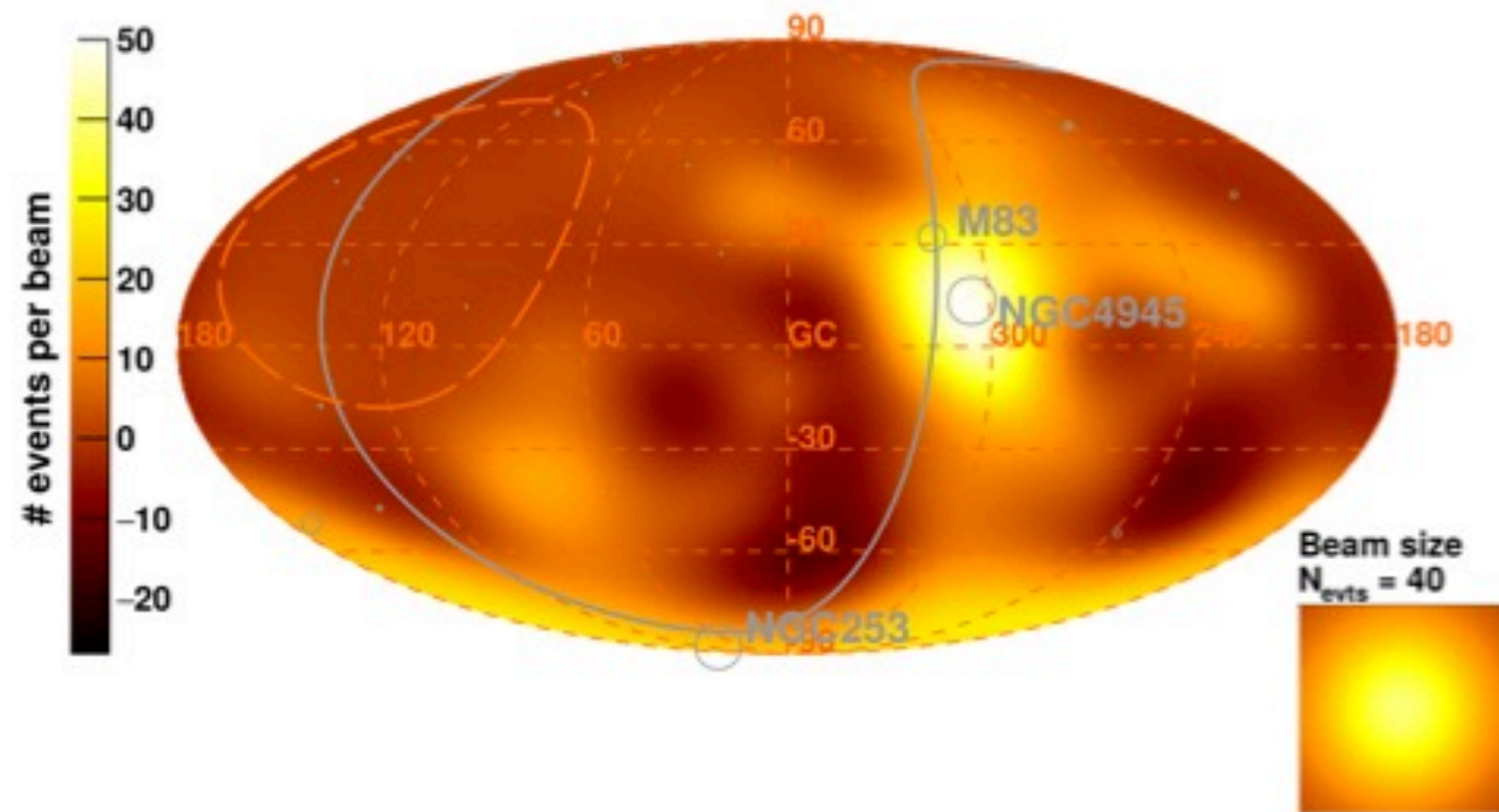
✦ AGNはAttenuation を考慮すると、近傍のCen Aに限定されて相関が大きくなる

Figure 2. TS profile above 39 EeV (*Top*) and 60 EeV (*Bottom*) over the fit parameters for SBG-only and γAGN-only models (*Left*) and for composite models including both SBGs and γAGNs with the same free search radius (*Right*). The lines indicate the 1−2σ regions.
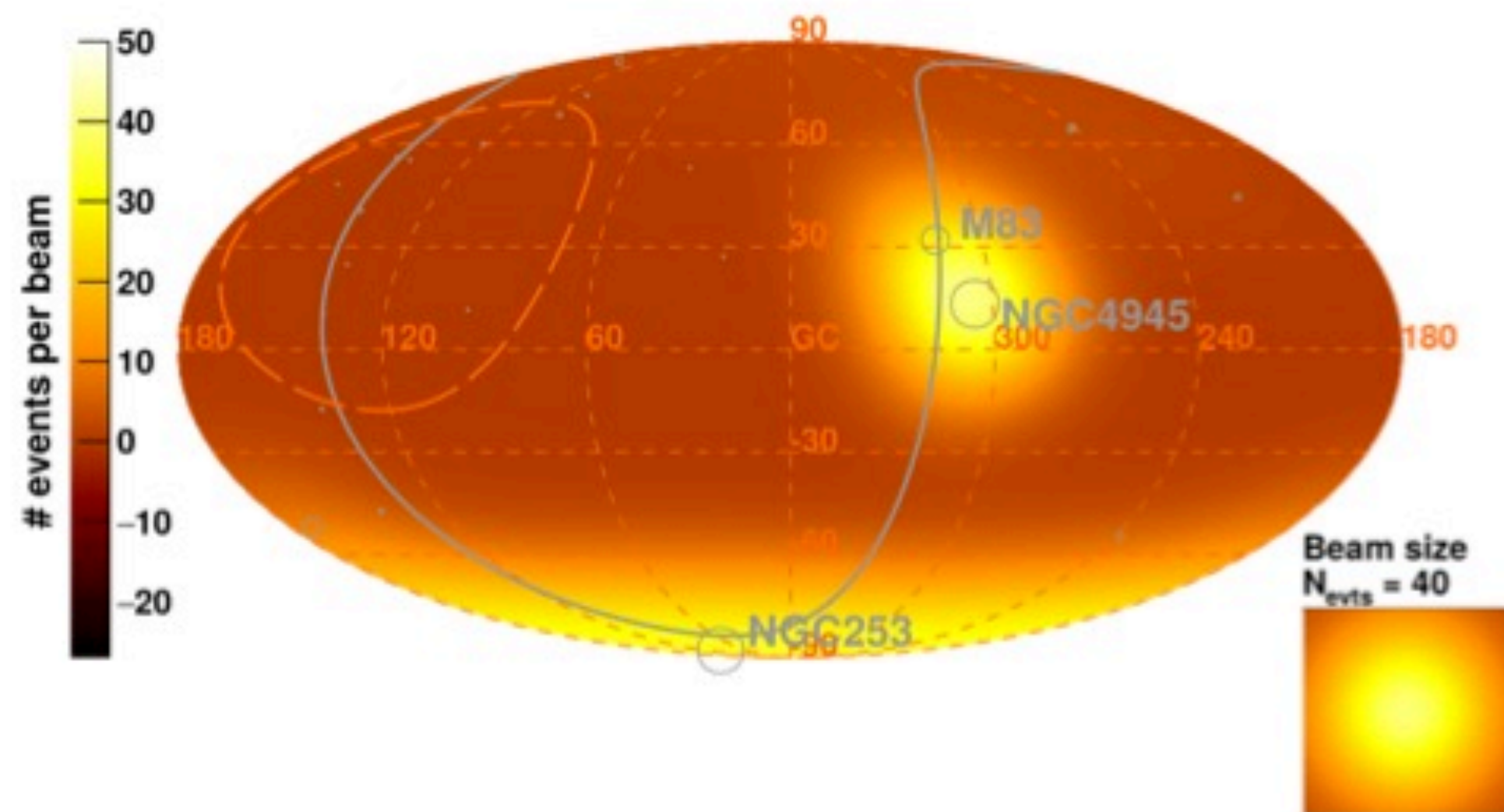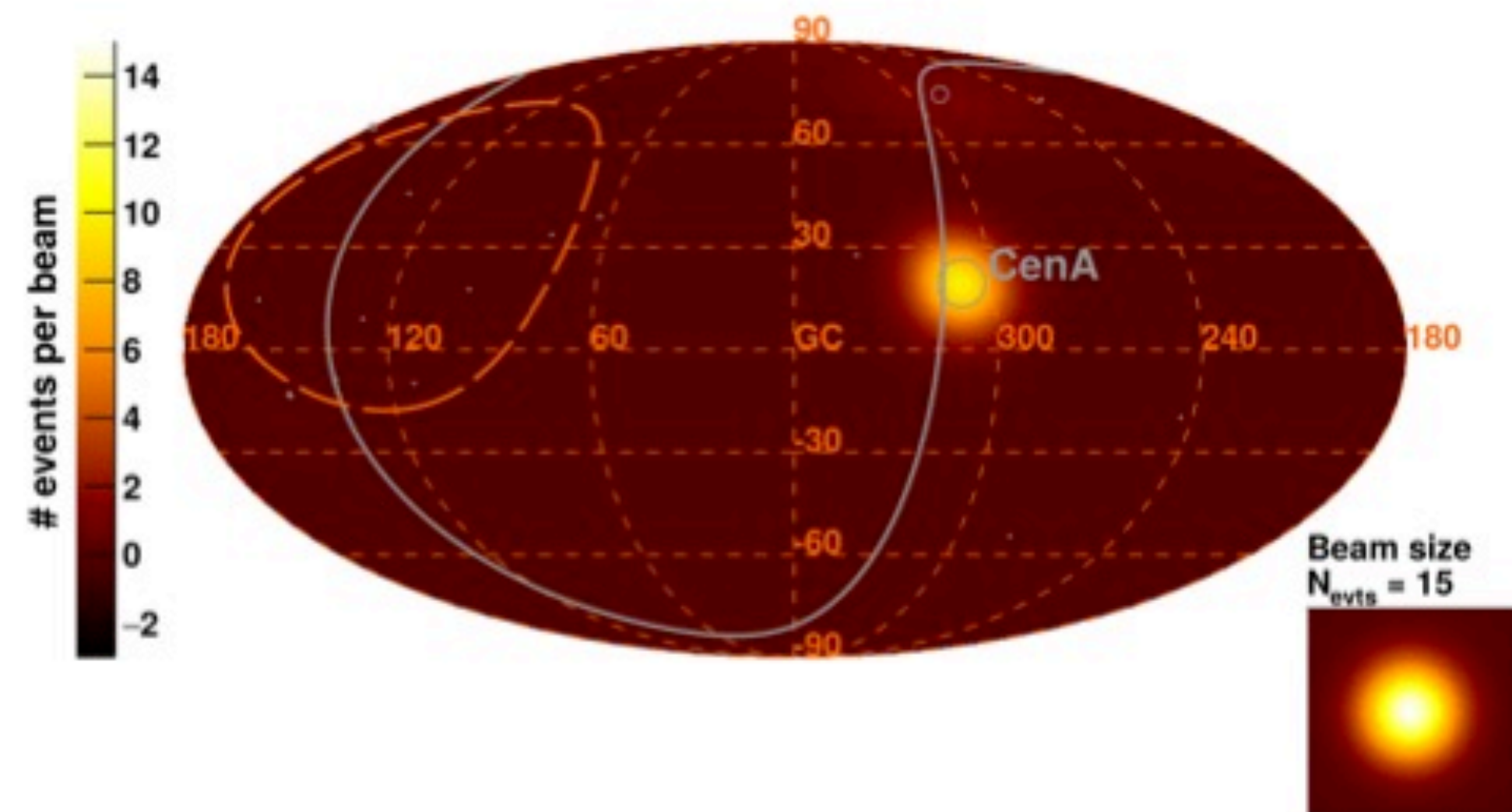
Best fit results

Observed Excess Map - E > 39 EeV

Observed Excess Map - E > 60 EeV
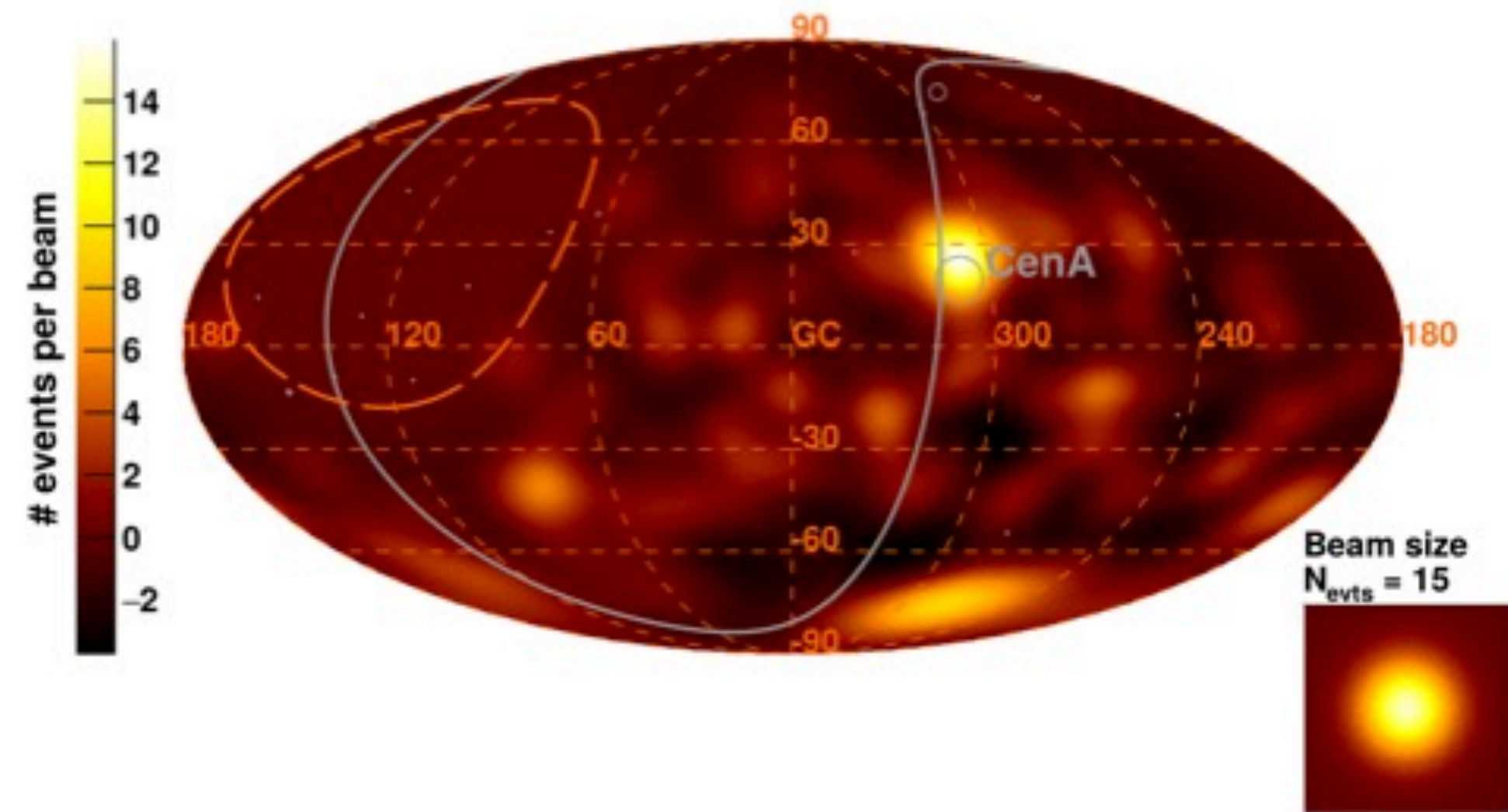
Model Excess Map - Starburst galaxies - E > 39 EeV

Model Excess Map - Active galactic nuclei - E > 60 EeV

Table 1. Results - Scenario A

Test hypothesis	Null hypothesis	Threshold energy[a]	TS	Local p-value $\mathcal{P}_{\chi^2}(\mathrm{TS}, 2)$	Post-trial p-value	1-sided significance	AGN/other fraction	SBG fraction	Search radius
SBG + ISO	ISO	39 EeV	24.9	3.8×10^{-6}	3.6×10^{-5}	$4.0\,\sigma$	N/A	9.7 %	12.9°
γAGN + SBG + ISO	γAGN + ISO	39 EeV	14.7	N/A	1.3×10^{-4}	$3.7\,\sigma$	0.7 %	8.7 %	12.5°
γAGN + ISO	ISO	60 EeV	15.2	5.1×10^{-4}	3.1×10^{-3}	$2.7\,\sigma$	6.7 %	N/A	6.9°
γAGN + SBG + ISO	SBG + ISO	60 EeV	3.0	N/A	0.08	$1.4\,\sigma$	6.8 %	0.0 %[b]	7.0°
Swift-BAT + ISO	ISO	39 EeV	18.2	1.1×10^{-4}	8.0×10^{-4}	$3.2\,\sigma$	6.9 %	N/A	12.3°
Swift-BAT + SBG + ISO	*Swift*-BAT + ISO	39 EeV	7.8	N/A	5.1×10^{-3}	$2.6\,\sigma$	2.8 %	7.1 %	12.6°
2MRS + ISO	ISO	38 EeV	15.1	5.2×10^{-4}	3.3×10^{-3}	$2.7\,\sigma$	15.8 %	N/A	13.2°
2MRS + SBG + ISO	2MRS + ISO	39 EeV	10.4	N/A	1.3×10^{-3}	$3.0\,\sigma$	1.1 %	8.9 %	12.6°

[a] For composite model studies, no scan over the threshold energy is performed.

[b] Maximum TS reached at the boundary of the parameter space.
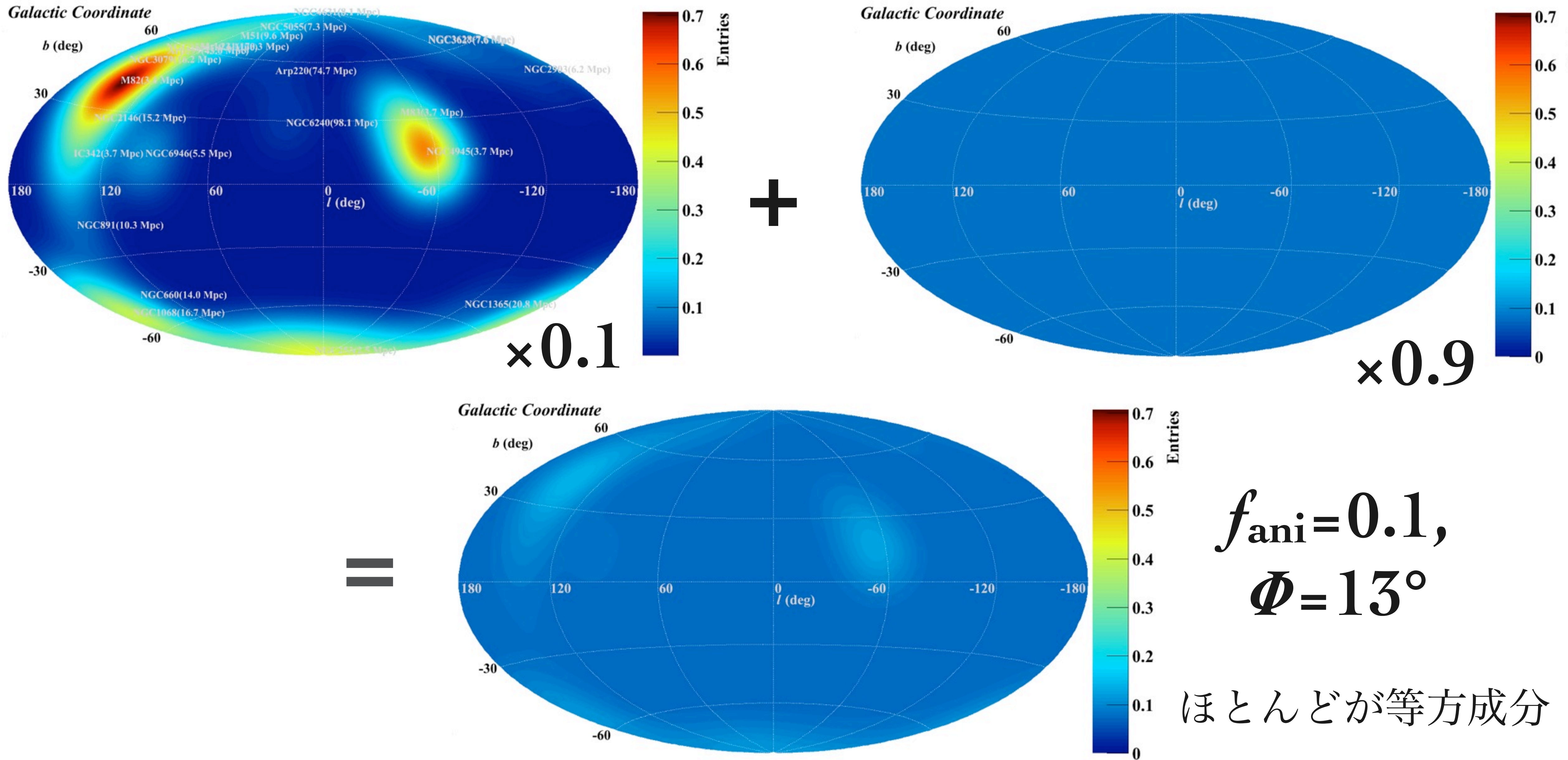
ISO: isotropic model.

✦ Warmspot: Cen A (AGN), M83 and NGC4945 (SBG)

    ✦ Galactic south pole: NGC1068 (SBG), NGC253 (SBG)

✦ Additional galaxies (Swift-BAT and 2MASS) are not favored

✦ Composite model: SBG contributions are dominated
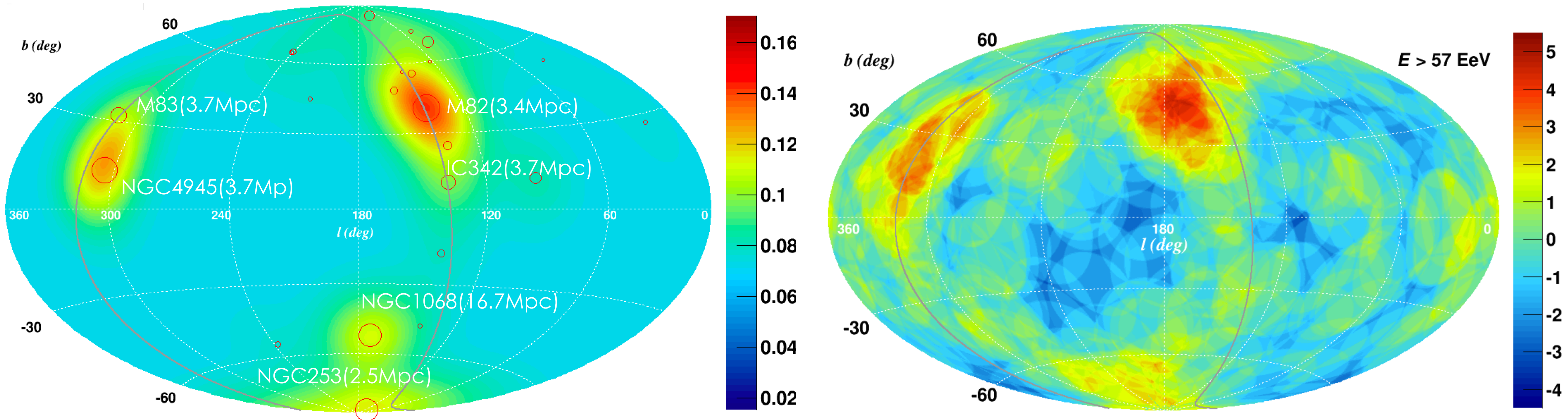
SBG flux pattern using best parameters of Auger

×0.1

+

×0.9

=

f_{ani}=0.1,
Φ=13°

ほとんどが等方成分

TA/Auger joint analysis?

Ugo Gia

¹Instituto
now at Ce
²Av. San M

銀河座標 (右端が0°)

✦ TA (7年分, 109事
Auger(10年分, 15

Auger best fit flux pattern of the starbur
$f_{ani} = 0.1, \Phi = 13°$

南半球では長

まとめ

✦ Augerで8 EeV以上の宇宙線の到来方向分布に持つダイポール構造が見つかった

　✦ Amplitudeが最大になる場所は、銀河中心から125°離れている。銀河系外起源の宇宙線を示唆している

　　✦ Amplitudeの大きさは、陽子から期待される値より小さい

　　　✦ (異方性から化学組成への制限がかかってきている）

✦ Flux patternでの相関解析

　✦ E > 39 EeVの到来方向分布は、SBGの異方性成分を10%と等方成分90%の場合に一致する

　　✦ 等方分布を4.0σで棄却

　✦ SBGと AGN or Swift-BAT or 2MRSを組み合わせ解析 (Composite model): SBGのFlux patternについて有意な相関を示す